Princeton Plasma Physics Laboratory

PPPL- 4873

PPPL- 4873

Three-dimensional, Impulsive Magnetic Reconnection in a Laboratory Plasma

S. Dorfman, H. Ji, M. Yamada, J. Yoo, E. Lawrence, C. Myers and T. Tharp

April, 2013

PPPL PRINCETON PLASMA PHYSICS LABORATORY

Prepared for the U.S. Department of Energy under Contract DE-AC02-09CH11466.

Princeton Plasma Physics Laboratory
Report Disclaimers

Full Legal Disclaimer

Trademark Disclaimer

PPPL Report Availability

Princeton Plasma Physics Laboratory:

http://www.pppl.gov/techreports.cfm

Office of Scientific and Technical Information (OSTI):

http://www.osti.gov/bridge

Related Links:

U.S. Department of Energy

Office of Scientific and Technical Information

Fusion Links

Three-dimensional, Impulsive Magnetic Reconnection in a Laboratory Plasma

S. Dorfman, H. Ji, M. Yamada, J. Yoo, E. Lawrence, C. Myers, and T. D. Tharp

Center for Magnetic Self-Organization,

Princeton Plasma Physics Laboratory, Princeton, New Jersey, USA

Abstract

Impulsive, local, 3-D reconnection is identified for the first time in a laboratory current sheet. The events observed in the Magnetic Reconnection Experiment (MRX) are characterized by large local gradients in the third direction and cannot be explained by 2-D models. Detailed measurements show that the ejection of flux rope structures from the current sheet plays a key role in these events. By contrast, even though electromagnetic fluctuations in the lower hybrid frequency range are also observed concurrently with the impulsive behavior, they are not the key physics responsible. A qualitative, 3-D, two-fluid model is proposed to explain the observations. The experimental results may be particularly applicable to space and astrophysical plasmas where impulsive reconnection occurs.

PACS numbers: 52.35.Vd, 52.72.+v

Magnetic reconnection is a fundamental plasma process involving the efficient conversion of magnetic field energy to plasma kinetic energy through changing field line topology. Reconnection has been observed in a variety of contexts [38] including the solar surface [26, 28, 32], the Earth's magnetotail [3, 10], and tokamak plasmas [18, 33, 36]. In all these cases, reconnection is not only fast, but also impulsive; in other words, a slow buildup phase is followed by a comparatively quick release of magnetic energy. Signatures of impulsive behavior have been previously identified in laboratory reconnection experiments [17, 19, 35].

An open question in the literature is if this behavior can be described by a two-dimensional model with no spatial variation in the out-of-plane (y) direction or if impulsive reconnection is fundamentally three-dimensional. While two-dimensional, impulsive reconnection models exist, these models may be modified by the presence of a third dimension. For example, the reconnection rate spikes when secondary magnetic islands are ejected in 2-D simulations [6], but in 3-D runs these islands become flux ropes with complex structure in the third dimension [7]. In 2-D systems there is a clear X-point where impulsive reconnection may take place, but in 3-D, fast reconnection could take place at all points along the X-line simultaneously or spread in the out-of-plane direction. Evidence for the later view is suggested by space measurements, including the spread of fast reconnection signatures in the out-of-plane direction during magnetospheric substorms [23] and in a cascade of solar coronal loops [12]. The addition of 3-D variation also allows for a large class of wave modes with finite k_y; these modes have long been considered as a possible source of anomalous resistivity that may speed up reconnection [2, 4, 5, 8, 17, 34].

In this letter, localized current disruptions are identified in the Magnetic Reconnection Experiment (MRX) as the first example of fast, impulsive, and *fundamentally three-dimensional* local magnetic reconnection in a laboratory current sheet. Signatures of flux ropes are found in the reconnecting current layer. The observed disruptions are due to the ejection of these 3-D, high current density regions associated with O-points at the measurement location. By contrast, magnetic fluctuations, long considered as a possible cause of anomalous resistivity, are not the key physics responsible for the observed impulsive phenomena.

Experiments are performed on the Magnetic Reconnection Experiment (MRX), a well-controlled and well-diagnosed driven laboratory experiment [37]. Two donut-shaped flux cores produce the plasma and drive the reconnection. In the pull phase of the discharge

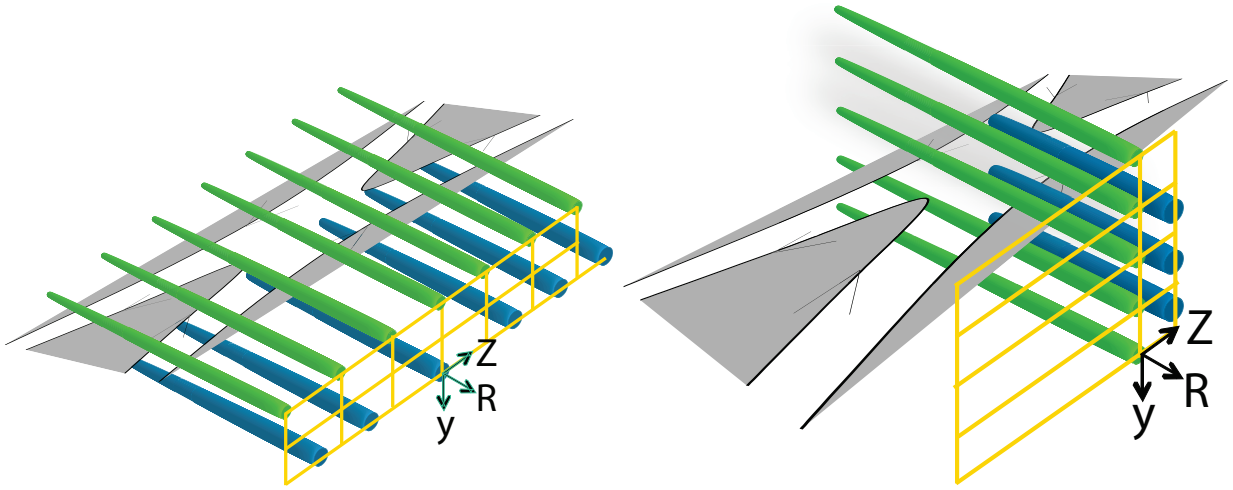

FIG. 1: Probe locations in the current sheet for in-plane measurements (left) and out-of-plane measurements (right). The local coordinate system is indicated by the coordinate axes in both plots. The Cartesian coordinate y is locally oriented in the azimuthal direction of MRX. For illustration purposes, parts of the reconnection plane are shaded gray. In the left panel, seven fine structure magnetic field probes (light green), each with 35 magnetic sensors, are located in the $y = 0$ plane on both sides of the current sheet. In the right panel, five fine structure probes, each with 50 magnetic sensors, are located at $Z = 0$, but at various out-of-plane y positions. Probes in both setups are separated by 3 cm. Additional probes to measure density, temperature, or high frequency magnetic field fluctuations may be placed nearby in the blue positions.

studied here, a current sheet forms in the plasma as a result of decreasing the current in the flux cores. No external guide field is applied in the present experiments. Also unlike prior studies of reconnection between externally generated 3-D flux ropes [16, 21], flux ropes may be spontaneously generated in the MRX current sheet geometry. Additional details of the experimental setup are described elsewhere [9, 37]; for the purposes of this letter, the reconnection region in a localized toroidal section of the device is considered. This region is illustrated in Fig. 1; R is the inflow direction, Z is the outflow direction, and y is a Cartesian coordinate locally oriented in the azimuthal direction. Two probe setups are shown: one for measurements in the reconnection plane (left) and one to measure variation in the out-of-plane (y) direction (right). This approach differs significantly from *Katz et al.* [19] which models impulsive reconnection with a guide field as a global (i.e. periodic in the third direction) rather than a local phenomena. While global impulsive reconnection may

be more applicable to tokamak sawteeth and reverse-field pinches where similar periodicity is observed [31, 36], the present study is more relevant to space and astrophysical plasmas which have no such periodicity [11]. At the time of the observed disruptions, typical plasma parameters are $n_e \sim 10^{13}$ /cm^3 and $T_e \sim 5$ eV. This gives a mean free path of 5 cm for electron-ion collisions, which is larger than the typical current sheet width of 1–2 cm; thus the MRX layers at the disruption time are considered to be collisionless.

Data gathered using the in-plane setup from Fig. 1 well-illustrates the basic features of a current layer disruption, defined as an event where the current density drops and the inductive electric field peaks. Discharges are prepared using a set of parameters that have been experimentally found to lead to current layer disruptions at the y location of the measurements. From a few hundred identically prepared discharges, cases with a clear disruption at the probe location are selected using strict quantitative criteria, such as those outlined in the caption of Fig. 3. On average, one out of every three cases meet the criteria, for a total of over 100 disruptive discharges in each experimental setup. While there is considerable variation in the details of each disruptive discharge, the key features discussed in this paper are common to nearly all discharges that meet the quantitative criteria for a disruption. One such discharge is shown in Fig. 2. As illustrated in Row A, the total out-of-plane current is initially 8 kA, but drops by 3 kA within about 4 μs around $t = 332$ μs. This timescale for the out-of-plane current drop is comparable to an ion cyclotron time of ~ 4 μs obtained from the upstream reconnecting field at $t = 332$ μs. At the same time, the electric field rises from 2 V/cm to over 4 V/cm as the reconnection rate spikes. This inductive electric field at the X-point is obtained through integration of magnetic flux; error from toroidal asymmetry associated with disruptive discharges is estimated at no more than 10% [9].

The details of the layer structure for this discharge reveal that the disruption is due to the ejection of a high current density O-point structure from the layer. Each of the three panels in Rows B, C, and D of Fig. 2 represent a time indicated by a vertical dashed line in Row A. The height of the contours in Row B (equivalent to the color in Row C) shows the out-of-plane current density moving outward in Z over the course of the disruption. One of these areas of high current density has a clear O-point structure as illustrated by the flux contours and B_R measurements shown in Rows C and D. At $t = 330$ μs, just before the total current drops, B_R as a function of Z at the R location of the X-point shows two clear

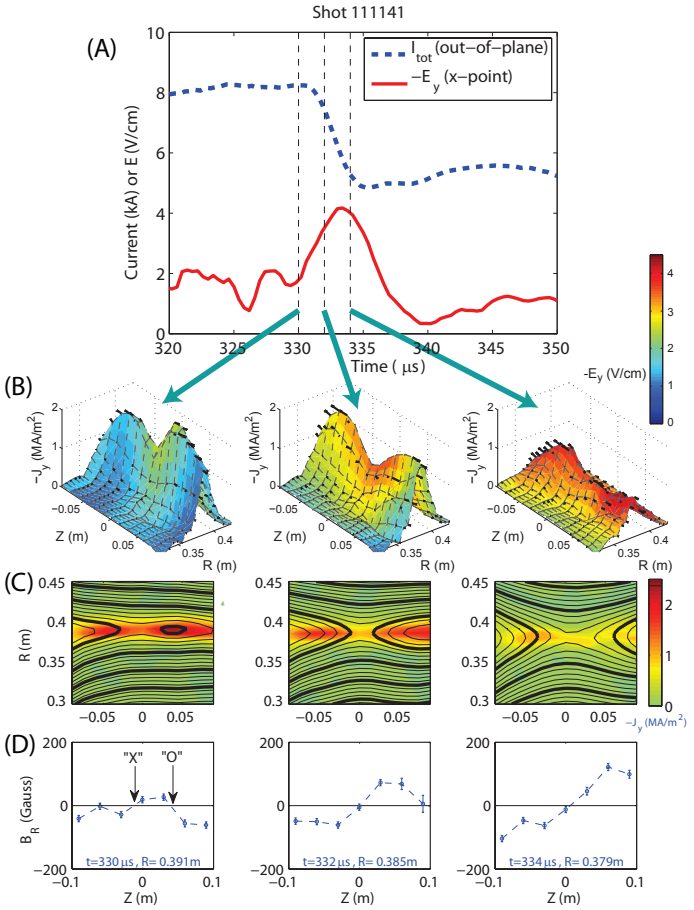

FIG. 2: An example of a current layer disruption in which the electric field peaks and the current drops as a flux rope structure is ejected from the layer. Row A: total out-of-plane current drop and reconnection rate enhancement during a current layer disruption. Shown are the total out-of-plane current integrated over the field of view of the fine structure array (thick dashed line) and inductive electric field at the X-point (solid line) for a representative deuterium discharge at 8 mTorr. Row B: detailed layer profiles from the fine structure magnetic field probes for the three times indicated by the vertical dashed lines in the top panel. The height of the contours represents out-of-plane current density $-J_y$ obtained though differentiation of 2-D magnetic field data, the color scale inductive electric field $-E_y$, and the arrows in-plane current derived from the out-of-plane magnetic field. Row C: Flux plots with current density shaded for the same three times. Row D: B_R as a function of Z at the R location of the current sheet center as measured by the fine structure probe array. As the disruption proceeds, the layer aspect ratio decreases; at the same time, B_R increases, first near $Z = 0$ and then at outer Z locations. An X and O-point for the first time slice are marked on the figure.

zero crossings, identified as the X and O-points on the figure. Consistent with this, the corresponding flux plot clearly shows the O-point associated with the flux rope structure. A third zero crossing is not well resolved, but suggests a possible second flux rope at $-Z$. To avoid confusion with the various definitions of flux ropes that appear in the literature, a "flux rope" is defined here as a 3-D, high current density region associated with an O-point at the measurement location. Inside a flux rope, density is peaked and an enhanced core field may be observed. Since these additional signatures are not always clear, it is important to note that the definition presented here differs from the most rigorous definitions of a flux rope (e.g. *NRC* [24]) found in the literature.

Current disruptions occur in discharges with strong local 3-D asymmetry in the pull phase initial condition. This may be seen by examining data from the stacked probe configuration on the right side of Fig. 1. Positive y, which points downward, approximates the out-of-plane electron flow direction within the layer. At the toroidal location of the measurements, gradients of the equilibrium density and magnetic field in the y direction are a key feature of the initial condition of the MRX pull phase; these gradients have a typical scale length only one order of magnitude greater than the width of the layer. This average behavior is shown in the left panel of Fig. 3 for the density at the center of the layer and the upstream magnetic field B_{sh} at a time near the start of the pull phase of the discharge, prior to the disruption and before flux rope formation. Data is averaged over discharges with a clear disruption, selected using the thresholds explained in the figure caption. In the right panel, density and magnetic field are displayed during a later portion of the pull period by which time the disruption has already taken place and the original gradient in the upstream magnetic field has relaxed.

To better understand the role of these gradients, the out-of-plane magnetic field profile in the R-y plane is examined as a function of time for an example discharge in Fig. 4. A buildup phase occurs during the time period shown by the first row of plots; the green region where magnetic field is small visibly narrows, especially at smaller y, indicating an increase in current density. The region in which this buildup occurs is typically characterized by a density gradient in the electron flow ($+y$) direction, consistent with a buildup mechanism similar to the layer sharpening described by *Huba and Rudakov* [15]. The second row of plots shows the disruption phase; the green region broadens, first at small y by $t = 331.6$ μs and then at large y by $t = 333.2$ μs. Thus the disruption process is not uniform in y, but

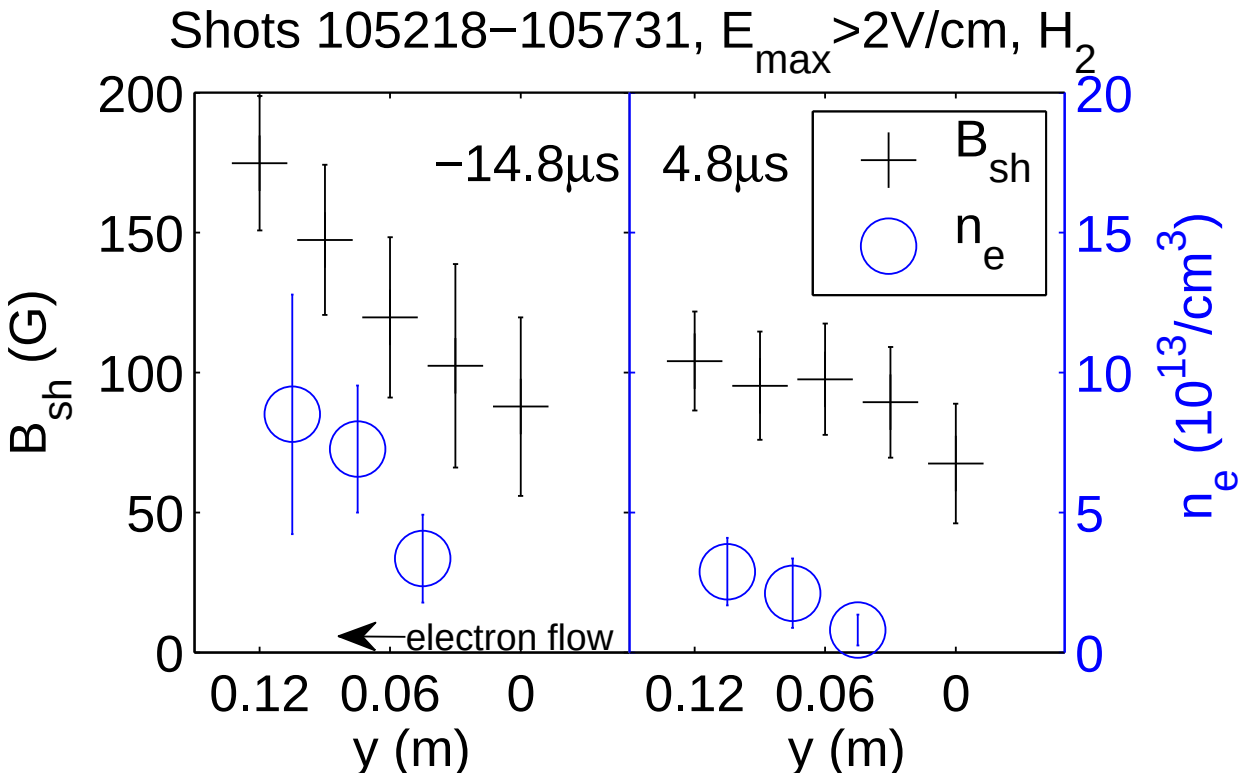

FIG. 3: Probe measurements of out-of-plane gradients before a current layer disruption and prior to flux rope formation (left) and after the disruption (right). Black crosses represent the upstream magnetic field obtained from fitting the experimental data to a Harris profile [13] in the inflow region at $Z = 0$. Blue circles show density measured at the current sheet center at $Z = 2.6$ cm. Data are averaged over 101 hydrogen discharges at 10.8 mTorr with a peak inductive electric field of at least 2 V/cm at $y = 6$ cm. The time indicated in the upper portion of each panel is with respect to the disruption time. In the pull phase initial condition, there are strong gradients in both quantities in the out-of-plane electron flow ($+y$) direction. Following the disruption, the original magnetic field gradient has relaxed and density is lower.

rather spreads in the electron flow ($+y$) direction. The time evolution of these y gradients of B_z is related to the flux rope structures observed in the in-plane measurements. When a flux rope builds up at or passes by the location of the probes stacked at $Z = 0$, the layer narrows. Once the flux rope is ejected past the Z location of the stacked probes, the layer is seen to broaden and disrupt.

While 3-D flux ropes are analogous to 2-D islands, several key features of the observed

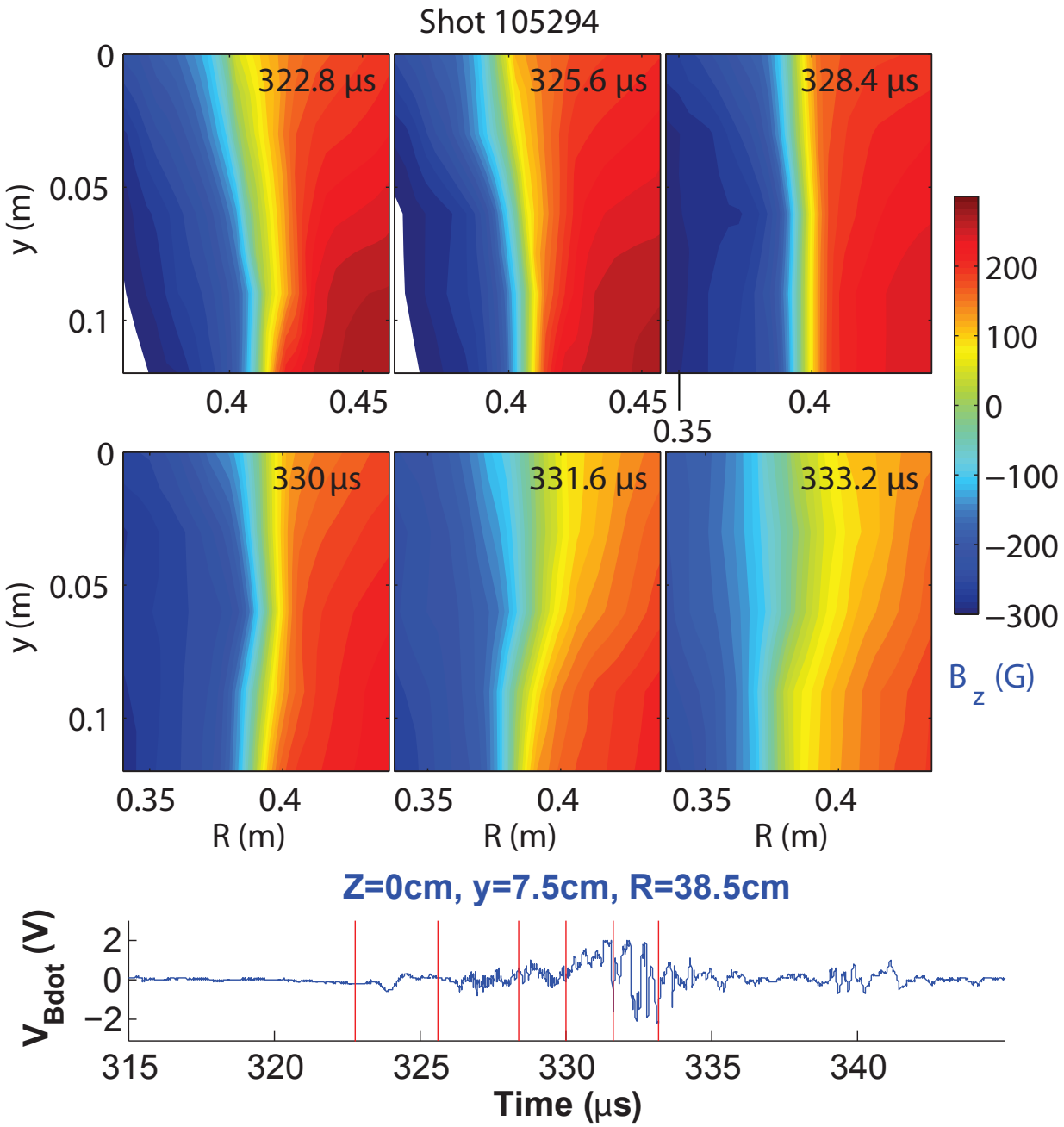

FIG. 4: Out-of-plane view of current density increase and subsequent disruption. Magnetic field B_z is plotted at six times as a function of R and y for an 8.5 mTorr deuterium discharge. The top row shows the buildup phase with time increasing to the right while the second row shows the disruption. Note that the disruption spreads from top to bottom in the electron flow ($+y$) direction. Also shown in the bottom panel of the figure is a plot of magnetic fluctuations measured at $Z = 0$ cm, $y = 7.5$ cm, $R = 38.5$ cm with the six times for the upper plots indicated by vertical red lines.

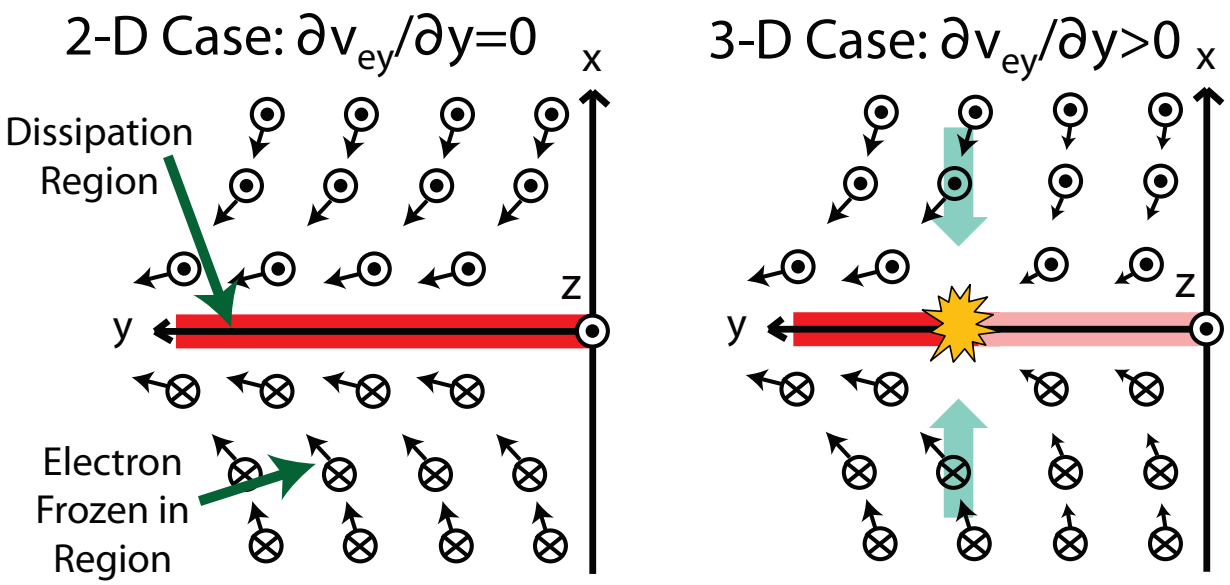

FIG. 5: Diagram of the inflow region showing electron flow (arrows) convecting field line (circles) towards the dissipation region (red shaded region) in both the 2-D case with no spatial variation in the out-of-plane direction (left) and a simplified 3-D case with an out-of-plane electron flow gradient (right) associated with added y variation of B_x. B_x is not shown explicitly, but the resulting modifications to the flow pattern and current density in the 3-D case are. For example, lighter shading represents lower current density in the dissipation region due to larger $\partial B_x/\partial z$. The 3-D variation shown may lead to a layer disruption as described in the text.

current disruptions have no clear 2-D analogue. For example, strong out-of-plane gradients are consistently observed in disruptive discharges; this association cannot be explained by a 2-D model. Similarly, the spreading of the disruption in the y direction requires 3-D physics to explain. Finally, magnetic fluctuations in the lower hybrid frequency range with finite k_y are observed concurrently with disruptions (see, for example, the bottom panel of Fig. 4). Although these fluctuations have characteristics consistent with *Ji et al.* [17], the observed out-of-plane gradients and flux rope structures are not predicted by a picture in which small-scale fluctuations are responsible for a locally enhanced reconnection rate. Therefore, neither a 2-D model nor an anomalous resistivity model is capable of explaining the observations. The key features of the disruption imply a fundamentally three-dimensional process.

This leads to an important question: How do these 3-D features lead to the observed disruptions? While this is still a subject of active research, with some physical intuition

it is possible to construct a simplified model consistent with the observations. This 3-D two fluid model is built on the 2-D Hall MHD picture. Due to the two-scale structure of the diffusion region, there is a region where only electrons are frozen to the field and Hall MHD applies. Here, electrons and magnetic field move together while the slower ions control plasma density. The resulting configuration in the inflow region is schematically illustrated by the magnetic field lines (circles) and electron flow vectors (arrows) in the left panel of Fig. 5. Although frozen-in electron flow convects magnetic field B_z towards the red dissipation region in both the x and y directions, there is no y variation of the field or flow due to the symmetry constraint.

In 3-D, this same Hall physics may lead to disruptions. In the simplified physical picture shown in the right panel of Fig. 5, density is uniform, and the key difference from the 2-D case is the introduction of an out-of-plane electron flow gradient associated with magnetic field gradients (see figure caption for details). Under the charge neutrality assumption, electron flow continuity in the Hall MHD region demands that a nonzero and positive $\partial v_{ey}/\partial y$ be supported by an enhanced inflow of electrons and field from the outer edge of the Hall MHD region as indicated by the thick green arrows. As the dissipation region adjusts to this dynamical change, the reconnection rate is enhanced. The faster conversion of reconnecting field B_z to reconnected field B_x also self-consistently reduces v_{ey}, modifying the initial gradient, causing the disruption to spread in the electron flow direction within the layer. These 3-D two-fluid effects are similar in many ways to prior studies of "reconnection waves" and Hall MHD shocks [14, 15, 20, 29]. The proposed physical picture of the disruption may equivalently describe the propagation of the "reconnection wave" outlined by *Huba and Rudakov* [14]. In this case, the v_{ey} gradients and 3-D field line structure are not part of the initial condition; they are instead due to an externally imposed magnetic field perturbation.

Several key features of the proposed model agree well with MRX observations. For example, the model explains the observed peak in the reconnection rate, the disruption spreading in y, and the importance of the out-of-plane magnetic field gradient in the initial condition. Consistent with *Yamada et al.* [38], the enhanced inflow described by the model means that the Hall signatures will peak at the disruption time; measurements of the quadrupole magnetic field and electrostatic potential well (not shown) corroborate this prediction. Although the observed flux ropes are not explicitly included in the model discussed here, note that

the cut in Fig. 5 is taken at the Z location of the X-point. As the reconnection rate at the X-point peaks at a given y location, any flux ropes that have formed to the side of the X-point will necessarily be ejected outward, consistent with the picture of Fig. 2. This ejection process causes the gross magnetic topology change in Rows B and C of the figure that makes the disruption rather dramatic.

An important aspect of this proposed physical picture is that out-of-plane gradients locally drive the reconnection through the Hall term, and the dissipation region adjusts to produce impulsive behavior. This is in direct contrast to anomalous resistivity models where the key physics takes place inside the dissipation region and the outside regions adjust. Thus this new 3-D two-fluid picture is important because (1) it shows that the Hall terms which leads to steady-state fast reconnection in 2-D can lead to localized, fast, impulsive reconnection in 3-D and (2) it decouples impulsive phenomena from the detailed physics of the electron dissipation region, relegating magnetic fluctuations once thought to be directly responsible for fast reconnection to a less consequential role.

The observations presented in this paper may be particularly applicable to space and astrophysical plasmas where impulsive reconnection occurs. For example, observations of busty bulk flows in the magnetotail are consistent with 3-D bursts of spatially localized reconnection [30]. Other key features of 3-D impulsive reconnection observed in MRX also have possible analogues in space observations, including current disruptions [1, 22, 25], flux rope signatures [11], and electromagnetic fluctuations [27, 39]. Future multi-point satellite studies (e.g. Cluster and Magnetospheric Multiscale) could be used to examine the potential importance of gradients along the X-line. Thus, comparison with MRX observations may provide important clues to the nature of 3-D reconnection processes observed in the magnetotail [23, 30] and on the solar surface [12].

In summary, current disruptions are identified in the Magnetic Reconnection Experiment as a new local, 3-D way to quickly release magnetic energy. These disruptions are due to the ejection of 3-D, high current density flux rope structures. In these discharges, the initial condition of the MRX pull phase (prior to flux rope formation) is characterized by strong local gradients in the out-of-plane direction. Further underscoring the 3-D nature of the process, the flux ropes are not ejected from the layer at all y locations symmetrically; instead, the disruption appears to spread in the electron flow (y) direction. These features cannot be explained by either a 2-D or an anomalous resistivity model. Instead, a 3-D, two-

fluid model consistent with the observations is proposed as a possible disruption mechanism. Future work will focus on 3-D probe array measurements to more fully resolve the reported flux ropes, simulations to validate the proposed model, and comparison with flux ropes [11] and disruptions [25] reported in space observations.

Acknowledgments

The authors thank W. Daughton and V. Roytershteyn for many insightful discussions and R. Cutler and D. Cylinder for their excellent technical support. S. D. was supported by a DOE FES Fellowship and the NDSEG Fellowship Program. This work is supported in part by the NASA Geospace Science Program and contract number DE-AC02-09CH11466 with the US DOE.

---

[1] Baker, D. N., T. I. Pulkkinen, V. Angelopoulos, W. Baumjohann, and R. L. McPherron (1996), Neutral line model of substorms: Past results and present view, *J. Geophys. Res.*, *1011*, 12,975–13,010.

[2] Bale, S., et al. (2002), Observation of lower hybrid drift instability in the diffusion region at a reconnecting magnetopause, *Geophys. Res. Lett.*, *29*, 2180.

[3] Birn, J. (2011), Magnetotail dynamics: Survey of recent progress, in *The Dynamic Magnetosphere*, *IAGA Special Sopron Book Series*, vol. 3, edited by W. Liu, M. Fujimoto, and B. Hultqvist, pp. 49–63, Springer Netherlands.

[4] Carter, T., et al. (2002), Measurement of lower-hybrid drift turbulence in a reconnecting current sheet, *Phys. Rev. Lett.*, *88*, 015,001.

[5] Daughton, W. (2003), Electromagnetic properties of the lower-hybrid drift instability in a thin current sheet, *Phys. Plasmas*, *10*, 3103.

[6] Daughton, W., et al. (2006), Fully kinetic simulations of undriven magnetic reconnection with open boundary conditions, *Phys. Plasmas*, *13*(7), 072101.

[7] Daughton, W., et al. (2011), Role of electron physics in the development of turbulent magnetic reconnection in collisionless plasmas, *Nat. Phys.*, *7*(7), 539.

[8] Davidson, R., and N. Gladd (1975), Anomalous transport properties associated with the

lower-hybrid drift instability, *Phys. Fluids*, *18*, 1327.

[9] Dorfman, S. (2012), Experimental study of 3-d, impulsive reconnection events in a laboratory plasma, Ph.D. thesis, Princeton University.

[10] Dungey, J. (1961), Interplanetary magnetic field and the auroral zones, *Phys. Rev. Lett.*, *6*(2), 47.

[11] Eastwood, J. P., et al. (2007), Multi-point observations of the hall electromagnetic field and secondary island formation during magnetic reconnection, *J. Geophys. Res.*, *112*(A6), A06,235.

[12] Grigis, P. C., and A. O. Benz (2005), The evolution of reconnection along an arcade of magnetic loops, *The Astrophysical Journal Letters*, *625*(2), L143.

[13] Harris, E. (1962), On a plasma sheath separating regions of oppositely directed magnetic field, *Il Nuovu Cimento*, *23*, 115.

[14] Huba, J. D., and L. I. Rudakov (2002), Three-dimensional hall magnetic reconnection, *Phys. Plasmas*, *9*(11), 4435–4438.

[15] Huba, J. D., and L. I. Rudakov (2003), Hall magnetohydrodynamics of neutral layers, *Phys. Plasmas*, *10*(8), 3139–3150.

[16] Intrator, T. P., et al. (2009), Experimental onset threshold and magnetic pressure pile-up for 3D reconnection, *Nature Physics*, *5*, 521–526.

[17] Ji, H., et al. (2004), Electromagnetic fluctuation during fast reconnection in a laboratory plasma, *Phys. Rev. Lett.*, *92*, 115,001.

[18] Kadomtsev, B. (1975), Disruptive instability in tokamaks, *Sov. J. Plasma Phys.*, *1*, 389.

[19] Katz, N., et al. (2010), Laboratory observation of localized onset of magnetic reconnection, *Phys. Rev. Lett.*, *104*, 255,004.

[20] Lapenta, G., et al. (2006), Kinetic simulations of x-line expansion in 3d reconnection, *Geophys. Res. Lett.*, *33*(10), L10,102.

[21] Lawrence, E. E., and W. Gekelman (2009), Identification of a quasiseparatrix layer in a reconnecting laboratory magnetoplasma, *Phys. Rev. Lett.*, *103*, 105,002.

[22] Lui, A. T. Y., A. Mankofsky, C.-L. Chang, K. Papadopoulos, and C. S. Wu (1990), A current disruption mechanism in the neutral sheet - A possible trigger for substorm expansions, *Geophys. Res. Lett.*, *17*, 745–748.

[23] Nagai, T. (1982), Observed magnetic substorm signatures at synchronous altitude, *J. Geophys.*

Res., *87*(A6), 4405–4417.

[24] NRC (2004), *Plasma Physics of the Local Cosmos*, The National Academies Press, Washington, DC.

[25] Ohtani, S., et al. (1992), Initial signatures of magnetic field and energetic particle fluxes at tail reconfiguration: Explosive growth phase, *J. Geophys. Res.*, *97*(A12), 19,311.

[26] Parker, E. (1979), *Cosmical magnetic fields: their origin and their activity*, International series of monographs on physics, Clarendon Press.

[27] Pickett, J. S., et al. (2001), Plasma waves observed in the cusp turbulent boundary layer: An analysis of high time resolution wave and particle measurements from the Polar spacecraft, *J. Geophys. Res.*, *106*, 19,081–19,100.

[28] Priest, E., and T. Forbes (2000), *Magnetic reconnection – MHD theory and applications*, Cambridge U. Press, Cambridge, UK.

[29] Rudakov, L. I., and J. D. Huba (2002), Hall magnetic shocks in plasma current layers, *Phys. Rev. Lett.*, *89*, 095,002.

[30] Shay, M., et al. (2003), Inherently three dimensional magnetic reconnection: A mechanism for bursty bulk flows?, *Geophys. Res. Lett.*, *30*(6), 1345.

[31] Tharp, T. D., et al. (2010), Measurements of impulsive reconnection driven by nonlinear hall dynamics, *Phys. Plasmas*, *17*(12), 120,701.

[32] Tsuneta, S. (1996), Structure and dynamics of magnetic reconnection in a solar flare, *Ap. J.*, *456*, 840.

[33] von Goeler, S., et al. (1974), Studies of internal disruptions and $m = 1$ oscillations in tokamak discharges with soft x-ray techniques, *Phys. Rev. Lett.*, *33*, 1201.

[34] Wang, Y., et al. (2008), An analytic study of the perpendicularly propagating electromagnetic drift instabilities in the magnetic reconnection experiment, *Phys. Plasmas*, *15*(12), 122,105.

[35] Yamada, M. (2011), Mechanisms of impulsive magnetic reconnection: Global and local aspects, *Phys. Plasmas*, *18*(11), 111212.

[36] Yamada, M., et al. (1994), Investigation of magnetic reconnection during a sawtooth crash in a high-temperature tokamak plasma, *Phys. Plasmas*, *1*(10), 3269–3276.

[37] Yamada, M., et al. (1997), Study of driven magnetic reconnection in a laboratory plasma, *Phys. Plasmas*, *4*, 1936.

[38] Yamada, M., et al. (2010), Magnetic reconnection, *Rev. Mod. Phys.*, *82*, 603–664

[39] Zhou, M., et al. (2009), Observation of waves near lower hybrid frequency in the reconnection region with thin current sheet, *J. Geophys. Res.*, *114*(A2), A02,216.

The Princeton Plasma Physics Laboratory is operated
by Princeton University under contract
with the U.S. Department of Energy.

Information Services
Princeton Plasma Physics Laboratory
P.O. Box 451
Princeton, NJ 08543

Phone: 609-243-2245
Fax: 609-243-2751
e-mail: pppl_info@pppl.gov
Internet Address: http://www.pppl.gov